

Electronic Supporting Information

Electron Transfer and Surface Activity of NiCoP Wrapped MXene: Cathodic Catalysts for Oxygen Reduction Reaction

Hao Xie^{a,#}, Demin Jiang^{a,b,#}, Huina Chen^a, Xiaoshuang Ma^a, Xiaojin Liu^a, QiQi^a, Yuqiao Wang^{a,*}

^aResearch Center for Nano Photoelectrochemistry and Devices, School of Chemistry and Chemical Engineering, Southeast University, Nanjing 211189, China

*Corresponding author: Tel. & Fax +862552090621

E-mail address: yqwang@seu.edu.cn (Y. Wang).

Experimental section

Synthesis of $Ti_3C_2T_x$ MXene

$Ti_3C_2T_x$ MXene was achieved by selective etching of the Al layers from Ti_3AlC_2 (MAX) phases¹. LiF (1.6 g) was firstly added into HCl (20 mL) solution and then stirred at 40 °C for 15 min. After then Ti_3AlC_2 powders (1 g) were gradually added. The solution was kept stirring at 40 °C for 24 h in the oil bath. The muddy was gathered by centrifugation (3500 rpm) and rinsed with distilled water to adjust the pH. The obtained solution was dispersed in deionized water and subjected to ultrasonic treatment in a nitrogen atmosphere. Finally, the suspension is centrifuged and vacuum dried to obtain the $Ti_3C_2T_x$ nanosheets.

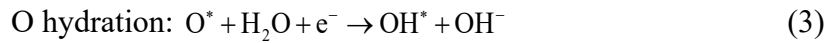
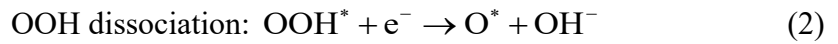
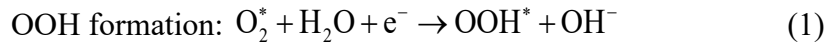
Analysis

The X-ray diffraction spectrum (XRD, Ultima IV) was applied to characterize the crystallinity of the synthesized samples in the 2-theta range of 5°- 80°. The X-ray photoelectron spectroscopy (XPS, K-Aepna, Thermo Fisher Scientific Inc., USA) was used to obtain the information of the

element composition and the surface chemical states of the obtained catalysts. Scanning electron microscope (SEM, FEI inspect F50), transmission electron microscope (SEM, JEM-2100F, JEOL, Japan) and high-resolution TEM (HRTEM, JEM-2100F, JEOL, Japan) were utilized to observe the surface morphology of the samples. Fourier transform infrared spectroscopy (FT-IR, Alpha-II, Bruker, Germany) was performed to analyze the functional groups on the surface of the materials.

DFT Calculation

The ORR process is considered into four elementary steps as follows²:



Note that * denoted the reaction site of materials. The free energy of reaction (1) – (4) can be calculated using Eqn (5)– (8).

$$\Delta G_1 = \Delta G_{\text{OOH}^*} - 4.92 \text{ eV} + \Delta G_{\text{pH}} + \text{eU} \quad (5)$$

$$\Delta G_2 = \Delta G_{\text{O}^*} - \Delta G_{\text{OOH}^*} + \Delta G_{\text{pH}} + \text{eU} \quad (6)$$

$$\Delta G_3 = \Delta G_{\text{OH}^*} - \Delta G_{\text{O}^*} + \Delta G_{\text{pH}} + \text{eU} \quad (7)$$

$$\Delta G_4 = -\Delta G_{\text{OH}^*} + \Delta G_{\text{pH}} + \text{eU} \quad (8)$$

The Gibbs free energy (ΔG) of the absorbed intermediate on the DFT scale is calculated by Eqn (9)

$$\Delta G = \Delta E_{\text{DFT}} + \Delta \text{ZPE} - T\Delta S \quad (9)$$

where ΔE_{DFT} represents the total electronic energy obtained with DFT, ΔZPE is the zero-point-energy correction and ΔS stands for the entropy of the system obtained through vibrational-frequency

analysis. T is the temperature (298.15 K in this work).³ The adsorption free energy changes of these intermediates can be expressed as follow:

$$\Delta E_{\text{OH}^*} = E(\text{OH}^*) - E(*) - (E_{\text{H}_2\text{O}} - 1/2 E_{\text{H}_2}) \quad (10)$$

$$\Delta E_{\text{OOH}^*} = E(\text{OOH}^*) - E(*) - (2E_{\text{H}_2\text{O}} - 3/2 E_{\text{H}_2}) \quad (11)$$

$$\Delta E_{\text{O}^*} = E(\text{O}^*) - E(*) - (E_{\text{H}_2\text{O}} - E_{\text{H}_2}) \quad (12)$$

$E_{\text{H}_2\text{O}}$ and E_{H_2} are the calculated DFT energies of H_2O and H_2 molecules in the gas phase.⁴ The free energy change of H^+ is derived according to Eqn (13)

$$\Delta G_{\text{pH}} = k_{\text{B}} T \ln(10) \times \text{pH} \quad (13)$$

k_{B} is Boltzmann's constant, and $\text{pH} = 13$ for alkaline medium, U is the potential measured against the normal hydrogen electrode at standard condition. The rate-determining step (RDS) is the elementary reaction with minimum reaction free energy (Eq. 14), while the overpotential is the corresponding potential obtained by Eq. (15).

$$G^{\text{ORR}} = \min \{ \Delta G_1, \Delta G_2, \Delta G_3, \Delta G_4 \} \quad (14)$$

$$\eta^{\text{ORR}} = |G^{\text{ORR}}| / e - 1.23 \text{ V} \quad (15)$$

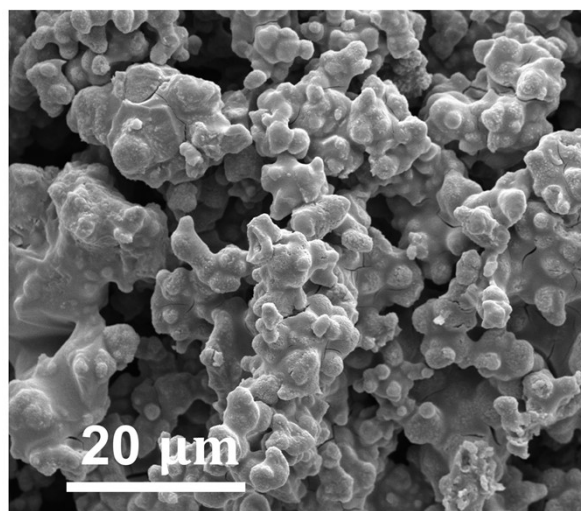


Fig. S1 SEM image of NiCoP.

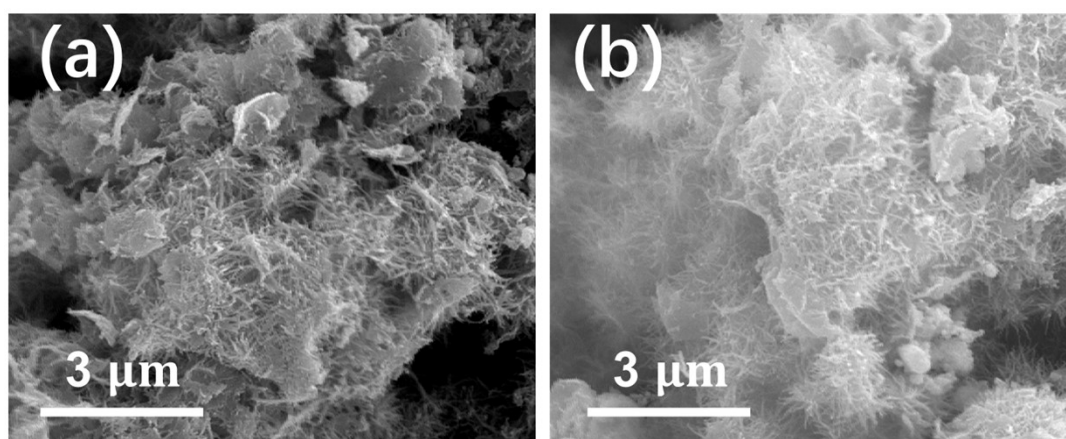


Fig. S2 The SEM images of MXene@NiCoP assembled electrodes before (a) and after 45 days tests(b).

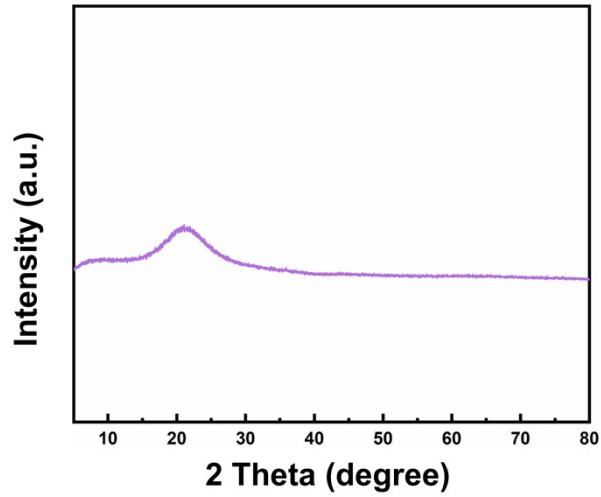


Fig. S3 XRD pattern of substrate material.

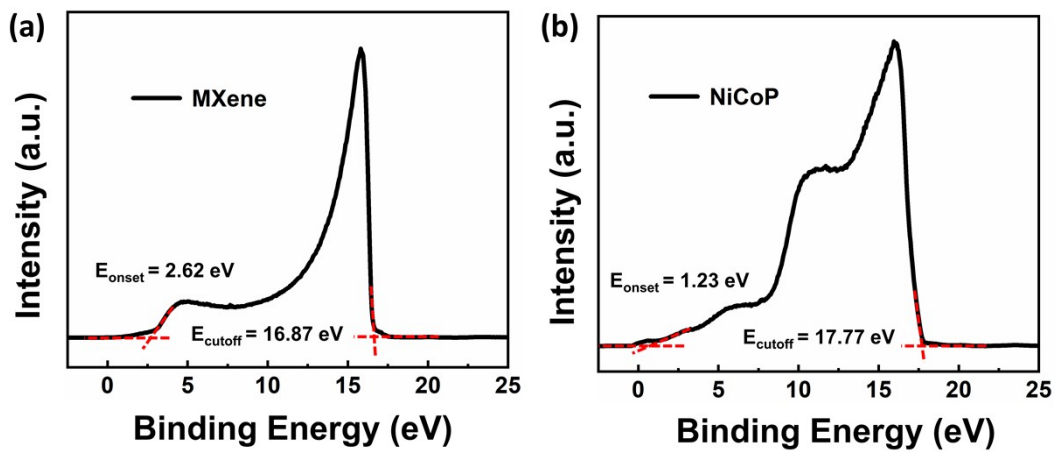


Fig. S4 UPS spectra of (a) MXene and (b) NiCoP.

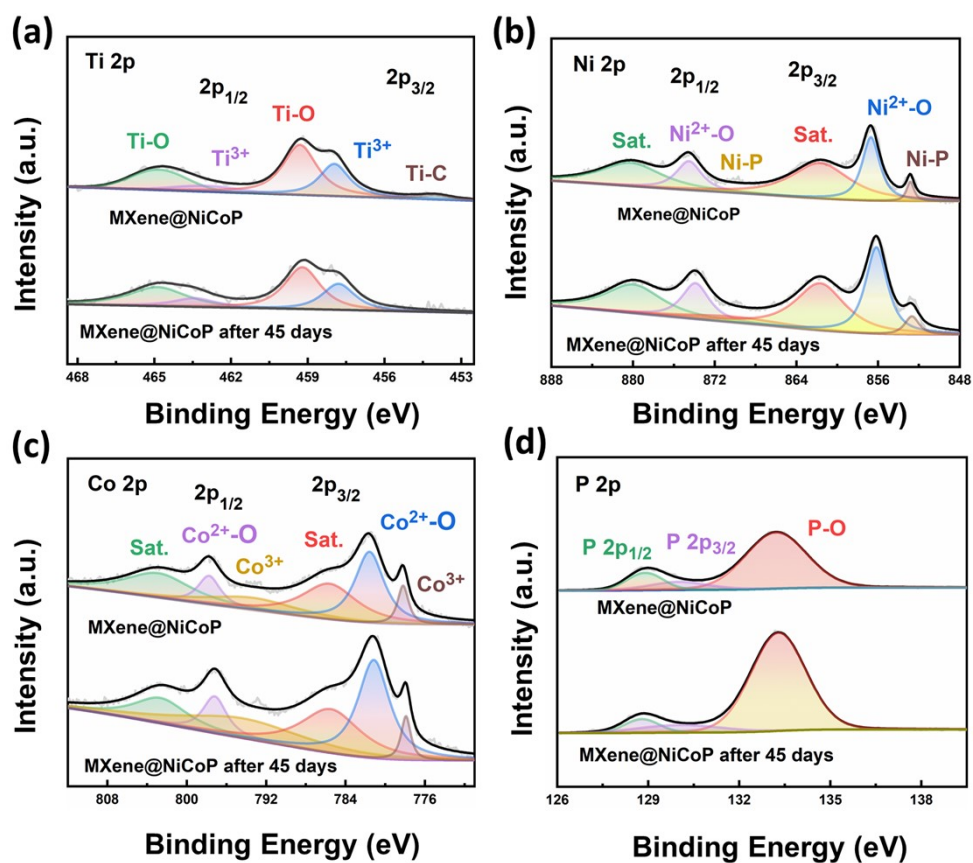


Fig. S5 XPS spectra of Ti 2p, Ni 2p, Co 2p, and P 2p of MXene@NiCoP and MXene@NiCoP after 45 days.

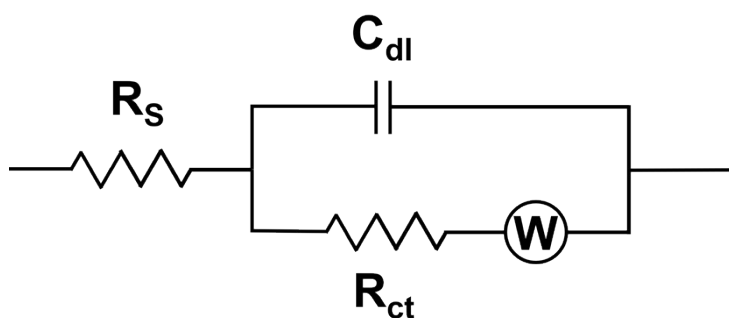


Fig. S6 The fitted equivalent circuit based on impedance data.

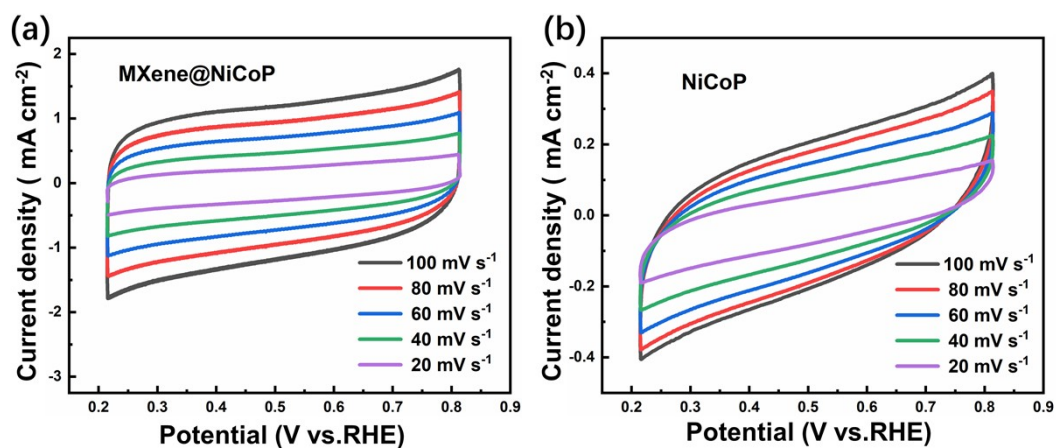


Fig. S7 CV curves of (a) MXene@NiCoP, (b) NiCoP.

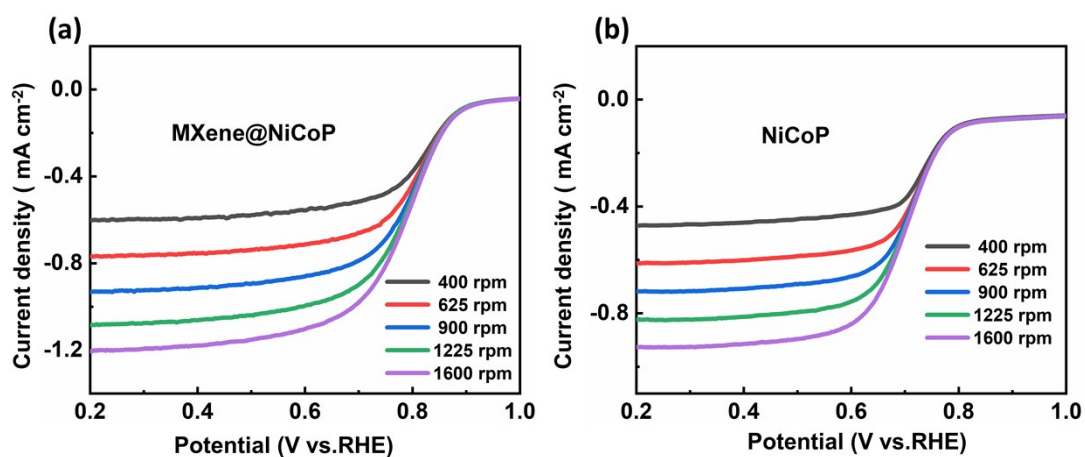


Fig. S8 RDE polarization curves of (a) MXene@NiCoP and (b) NiCoP.

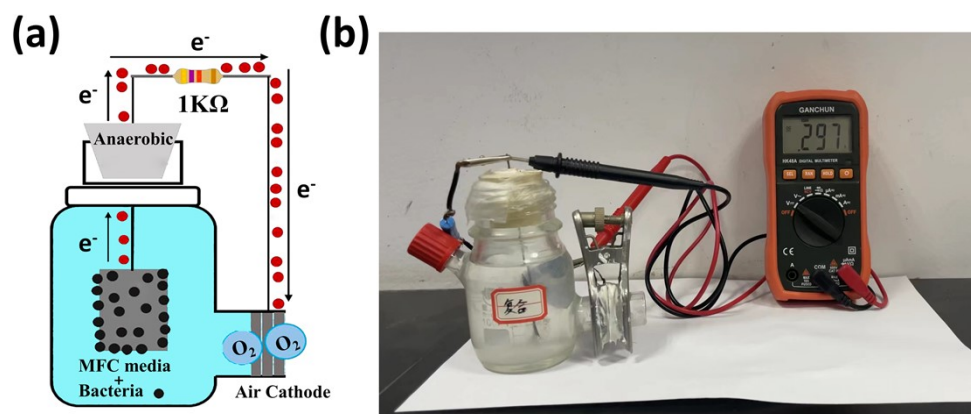


Fig. S9 The schematic diagrams of MFC device (a) and measurement (b).

Table S1. The simulated data from EIS.

Catalysts	R_s (Ohm cm^{-2})	R_{ct} (Ohm cm^{-2})	C_{dl} (10^{-7} mF cm^{-2})	Z_w (Ohm cm^{-2})
Pt/C	0.21	2.85	2.14	0.144
NiCoP	0.24	4.83	17.7	0.011
MXene@NiCoP	0.22	3.44	2.63	0.012

Table S2. The performance of air-cathode single-chamber MFCs equipped with the various ORR catalysts.

Catalyst	Cathode substrate	Anode substrate	Anode inoculum	P_{\max} (mW/m ²)	Ref.
MnO ₂ @Co ₃ O ₄	Stainless steel mesh	Carbon cloth	Anaerobic sewage	475	5
MOF-derived Fe-N/C	Carbon paper	Carbon felt	Anaerobic mixed bacteria	1232.9	6
NiFe-LDH@Co ₃ O ₄	Carbon cloth	Carbon felt	Activated sludge	467	7
N, P-PA-SS	Carbon cloth	Graphite brush	Sludge bacterial species	802	8
Co/Zeolite-GO	Carbon cloth	Carbon cloth	Activated sludge	600	9
Ti ₃ C ₂ /M _x O _y /Ag	Stainless steel mesh	Carbon felt	Activated sludge	418.1	10
CoNC-900	Stainless steel mesh	Carbon brush	Bacterial wastewater	1191	11
(Fe)/Fe ₃ O ₄ /FeS/NGC	Stainless steel mesh	Graphite fiber brush	Bacterial wastewater	930 ± 10	12
Ag, Fe-N-C	Carbon cloth	Carbon cloth	Anaerobic sludge	523± 7	13
3DHP Co-N-C	Carbon paper	Carbon paper	Activated sludge	427±8	14
NiCoAl-LDH	Stainless steel	Carbon felt	Anaerobic activated sludge	448.5 ± 12	15
GO/MgO	Carbon cloth	Carbon felt	Municipal sludge	755	16
MOF-derived Co-N-C	Carbon cloth	Carbon cloth	Activated sludge	400±10	17
V ₂ O ₅ -NR/rGO	Stainless steel mesh	Carbon cloth	Fish market wastewater	533 ± 37	18
CeO ₂	Carbon brush	Carbon cloth	Sodium acetate	840± 24	19
MN/NrGO	Carbon cloth	Carbon cloth	Anaerobic sludge	135.3	20
NPOMC	Carbon cloth	Carbon paper	Digester sludge	245.8	21

*NGC: nitrogen-enriched graphitic carbon, NPOMC: Nitrogen- and phosphorus-doped, ordered mesoporous carbon.MN: α -MnO₂ nanorods.

References

1. M. Naguib, V. N. Mochalin, M. W. Barsoum and Y. Gogotsi, *Adv Mater*, 2014, **26**, 992-1005.
2. C. C. Yang, S. F. Zai, Y. T. Zhou, L. Du and Q. Jiang, *Advanced Functional Materials*, **2019**, 1901949.
3. R. Ma, G. Lin, Y. Zhou, Q. Liu, T. Zhang, G. Shan, M. Yang and J. Wang, *npj Computational Materials*, 2019, **5**:78.
4. X. Zhang, Z. Xia, H. Li, S. Yu, S. Wang and G. Sun, *RSC Adv*, 2019, **9**, 7086-7093.
5. J. Chen, Y. Liu, J. Yang, H. Wang, H. Liu, S. Cao, X. Zhang, R. Wang, Y. Liu and Y. Yang, *Bioresour Technol*, 2022, **346**, 126584.
6. X. Luo, W. Han, W. Du, Z. Huang, Y. Jiang and Y. Zhang, *Journal of Power Sources*, 2020, **469**, 228184.
7. L. Jiang, J. Chen, D. Han, S. Chang, R. Yang, Y. An, Y. Liu and F. Chen, *Journal of Power Sources*, 2020, **453**, 227877.
8. F.-Y. Zheng, R. Li, S. Ge, W.-R. Xu and Y. Zhang, *Journal of Power Sources*, 2020, **446**, 227356.
9. A. Chaturvedi and P. P. Kundu, *ACS Appl Mater Interfaces*, 2022, **14**, 33219-33233.
10. X. Wang, X. Gong, L. Chen, S. Li, J. Xie and Y. Liu, *Catalysis Science & Technology*, 2021, **11**, 4823-4830.
11. S. You, X. Gong, W. Wang, D. Qi, X. Wang, X. Chen and N. Ren, *Advanced Energy Materials*, 2016, **6**, 1501497.
12. X. Xu, Y. Dai, J. Yu, L. Hao, Y. Duan, Y. Sun, Y. Zhang, Y. Lin and J. Zou, *ACS Appl Mater Interfaces*, 2017, **9**, 10777-10787.
13. B. L. Lai, Z. H. Xiao, P. Y. Jiang, Y. Xie, N. Li and Z. Q. Liu, *ChemElectroChem*, 2022, **9**, e202101699(1 of 9).
14. Q. R. Pan, P. Y. Jiang, B. L. Lai, Y. B. Qian, L. J. Huang, X. X. Liu, N. Li and Z. Q. Liu, *Chemosphere*, 2022, **291**, 132701.
15. J. Chen, J. Yang, L. Jiang, X. Wang, D. Yang, Q. Wei, Y. Wang, R. Wang, Y. Liu and Y. Yang, *Bioresour Technol*, 2021, **337**, 125430.
16. M. Li, S. Zhou and M. Xu, *Chemical Engineering Journal*, 2017, **328**, 106-116.
17. J.-C. Li, X.-T. Wu, L.-J. Chen, N. Li and Z.-Q. Liu, *Energy*, 2018, **156**, 95-102.
18. M. T. Noori, C. K. Mukherjee and M. M. Ghangrekar, *Electrochimica Acta*, 2017, **228**, 513-521.
19. L. Li, M. Wang, N. Cui, Y. Ding, Q. Feng, W. Zhang and X. Li, *RSC Advances*, 2016, **6**, 25877-25881.
20. R. K. Gautam, H. Bhattacharjee, S. Venkata Mohan and A. Verma, *RSC Advances*, 2016, **6**, 110091-110101.
21. Y. E. Song, S. Lee, M. Kim, J.-G. Na, J. Lee, J. Lee and J. R. Kim, *Journal of Power Sources*, 2020, **451**, 227816.